Original Article

TIPS Trends in Pharmaceutical Sciences 2019: 5(2): 93-102.

Preparation and Characterization of TiO_2-PEG NPs loaded with Doxorubicin

Zahra Sobhani[1,*], Reyhaneh Khademi[1], Mohammad Ali Behnam[2], Amin Reza Akbarizadeh[1]

[1]Department of quality control, School of pharmacy, Shiraz University of Medical Sciences, Shiraz, Iran.
[2]Nano Opto-Electronic Research Center, Electrical and Electronics Engineering Department, Shiraz University of Technology, Shiraz, Iran.

Abstract

Many chemotherapeutics used for cancer treatments show systemic toxicity during distribution to the normal tissues. Using nanoparticles (NPs) improves drug delivery efficiency and decreases the side effects of anticancer drugs. The aim of this study was to load doxorubicin (DOX) on TiO_2 NPs for their potential role in enhancing the anticancer efficacy of DOX while reducing its side effects. At first, for improving the dispersibility of TiO_2 NPs in water, the polyethylene glycol (PEG) with two MWs (1000 and 4000 kDa) was used for wrapping the surface of TiO_2 NPs. DOX was loaded on the TiO_2 NPs by forming complexes with titanium, to construct TiO_2-PEG-DOX NPs. The effects of various weight ratios of DOX to TiO_2 on the loading efficiencies of NPs were assessed. The stability of these NPs in two different pH values (7.4 and 5) was evaluated. At the end, the cytotoxicity of TiO_2-PEG-DOX was compared with free DOX against MCF-7 cell line. The formation of a thin layer of PEG around the TiO_2 NPs was confirmed through thermo gravimetric analysis and transmission electron microscopy techniques. Fluorescence scanning results showed the complex formation between DOX and TiO2-PEG. The loading efficiency of DOX in TiO_2-PEG1000 was 74% and in TiO_2-PEG4000 was up to 85%. These complexes were stable at different pH values for a long period (one month). The viability percent of cancerous cells exposed to TiO_2-PEG-DOX was lower than free DOX after 48 hr. The characteristics of TiO2-PEG-DOX showed that this drug delivery system is a promising strategy for future clinical practice.

Keywords: Doxorubicin, Drug delivery, Nanoparticle, Titanium dioxide.

1. Introduction

The advent of nanoparticles (NPs) in biomedical, bioengineering, and pharmacological fields made a revolution in delivering drugs. Nano-scale sizes of NPs enhance their potential to be attached and transported to cells (1, 2). Drug delivery by means of NPs promises a new technique to treat cancer cells efficiently without any major limitation and side effects (1, 2). Thus far, a variety of nano-structures such as mesoporous silica, graphene oxide, iron oxide (3), gold NPs (4), silver NPs (5, 6), and carbon nanotubes (7) have been successfully developed in drug delivery method. A desirable candidate for this method is titanium dioxide (TiO_2) NPs (8).

Concurrently, TiO_2 has shown some specific characteristics in pharmaceutical, and cosmetic industries and attracted a growing deal of interest to itself (9, 10). It is commonly considered to be biologically inert (11). TiO_2 is bio-friendly and has exceptional properties, such as good photo catalytic activity, high refractive index, and magnetic property (12-14). These characteristics of

Corresponding Author: Zahra Sobhani, Department of quality control, School of pharmacy, Shiraz University of Medical Sciences, Shiraz, Iran.
Email: sobhani@sums.ac.ir

Recieved: 27/03/2019; Accepted: 28/04/2019

TiO_2 derive from the spontaneous formation of an oxide layer on the titanium surface (15). TiO_2 can damage viruses, fungi, bacteria, and cancer cells (16) and can operate as an potent catalyzer for treating malignant cells (17, 18). Drug delivery, cell imaging, biosensors for biological assay, and genetic engineering are some types of biomedical application of TiO_2 NPs (2). TiO_2 NPs could be a good choice for biomedical applications as agents in dispensing drugs in drug delivery system, due to their availability (19), low-toxicity, good thermal conductivity, good optical absorption and chemical and thermal stability (2). TiO_2 nano-structures have been utilized in drug delivery systems for different anti-cancer drugs, such as temozolomide, doxorubicin, daunorubicin, and cisplatin (20-22). Biocompatibility of TiO_2 NPs could be increased by attaching polyethylene glycol (PEG) to their surfaces. PEGylation could help NPs to escape the Reticulo-Endothelial System (RES) and increase their half-life in blood circulation for passive targeting of the anticancer drugs to the tumor cells (16, 18).

Up to now, doxorubicin (DOX) is one of the effective anticancer drugs in treating cancers including ovarian carcinoma, lymphoblastic leukemia, breast carcinoma, and hepatocellular carcinoma (23). One of the greatest challenges for DOX is that "how to deliver this drug to the desirable spots". Therefore, a new delivery technique have been developed to reduce its side effects, which could change its bio-distribution and enhance its deposition at the tumor sites (3, 23). Chen *et al*. constructed a TiO_2-DOX NP as a drug delivery system, and the results showed that the anti-cancer efficacy of the drug per dose was productively increased in human SMMC-7721 hepato carcinoma cells (23). Besides, Ren *et al.* reported an enhanced DOX transport to breast cancer cells via TiO2 nano-carriers (21).

In the present study, TiO_2 NPs were evaluated as potent agents for drug delivery system. To enhance the dispersibility of TiO_2 NPs, a layer of PEG coated the mentioned NPs. After DOX loading on the TiO_2-PEG NPs, the efficacy of TiO_2-PEG-DOX NPs against cancerous cell line was assessed.

2. Material and methods

The TiO_2 NPs were purchased from Nanosany Company, Iran. The particle size of these NPs was reported 10-25 nm. Their purity was >99%, and their phase was anatase. PEG was obtained from Sigma-Aldrich, USA. DOX was obtained EBEWE Pharma, Austria. All other reagents were of analytical grade. The breast cancer cell line MCF-7 cells were provided by the National Cell Bank of Pasteur Institute (Tehran, Iran).

2.1. Preparation and characterization of TiO_2-PEG NPs

In order to improve the dispresibility and stability of TiO_2 NPs, polyethylene glycol (PEG, with three different molecular weights: 400, 1000, 4000) was used to enwrap the NPs. 25 mg TiO_2 NPs was suspended in 25 mL deionized water. After 30 min sonication, 250 mg PEG was added to the TiO_2 NPs suspension. The suspension was ultrasonicated for 30 minutes, and then stirred at room temperature overnight (5, 8). After being stirred, the suspension was centrifuged at 4000 rpm for 15 minutes to separate the unreacted TiO_2 NPs, and the supernatant was collected (5, 7). The formation of a polymer layer around the TiO_2 NPs was confirmed by the transmission electron microscopic image (TEM) (Philips Electron Optics, the Netherlands). Thermal analysis techniques including: Thermo-Gravimetric Analysis (TGA) and Differential Scattering Calorimetry (DSC), were carried out on these NPs by (METTLER TOLEDO, Swiss) under dynamic atmosphere of an inert gas (N_2) at 30 ml/min.

2.2. Preparation of TiO_2-PEG-DOX NPs

DOX loading on the TiO_2 NPs was performed through adsorption. For optimization drug loading, the effects of three factors were assessed: order of adding materials together, drug-carrier incubation duration time, and drug: carrier weight ratio.

2.2.1. Effect of order of adding substances on the drug loading

For evaluating the effect of PEG layer on the adsorption of DOX on the surface of TiO_2 NPs, the materials were added in two different orders.

In Method 1, TiO_2 NPs suspension in deionized water was sonicated for 30 minutes. Then PEG solution was added and sonicated for 30 minutes, again. After stirring for 24 hr, DOX solution was added to the TiO_2-PEG NPs and the final mixture was stirred overnight at ambient temperature. Drug loaded on the NPs were separated from the free drug molecules through centrifugation at 15000 rpm for 15 min at 4 °C and washed twice by deionized water to remove the unloaded drug molecules from TiO_2-PEG-DOX NPs. The amount of free DOX in the supernatant was analyzed by HPLC method (24-27).

For DOX analysis, the chromatographic system consists of a Hichrom C_{18} column (250×4 mm, UK) and a Cecil instrument (Adept series and CE 4200 UV/Vis Detector, England) was used. The mobile phase consisted of acetonitrile: distilled water (30:70 v/v) and the pH of the mobile phase adjusted to 3 using phosphoric acid. The flow rate was set to 1 mL/min and DOX was quantified at 233 nm. Validation of the HPLC assay demonstrated that this methodology was linear (r^2=0.9989) in the range of 0.312-5 µg/ mL of DOX. CV% was less than 8% and the accuracy was more than 92% within this range of concentrations (0.312-5 µg/ mL). The specificity was tested in presence of the NPs components.

In Method 2, similar first method, TiO_2 NPs suspension in deionized water was sonicated for 30 minutes. Then DOX was added and sonicated. At the end, PEG solution was added to the mixture. After sonicating for 30 min, the final mixture was stirred overnight at ambient temperature. Drug loaded on the NPs were analyzed as previous method.

2.2.2. Effect of DOX: TiO_2-PEG NPs incubation duration time on the drug loading

In order to investigate the interaction of DOX with TiO_2-PEG NPs, the fluorescence spectra of DOX and DOX-loaded TiO_2 NPs was studied. An aqueous dispersion of 10mg TiO_2 NPs, 100mg PEG4000 and 8mg DOX was sonicated and stirred on the magnetic stirrer. The fluorescence and UV spectra were then recorded at different reaction time intervals (0, 1, 2, 4 and 24 hr) using Hitachi F 2500 fluorescence spectrophotometer.

2.2.3. Effect of DOX: TiO2 NPs weight ratio on the drug loading

Different amounts of DOX and TiO_2 NPs were added together in the presence of PEG1000 or PEG4000 according to the Method 2. Drug loaded on the NPs were separated from the free drug molecule. The amount of free DOX in the supernatant was analyzed by HPLC method. Each formulation was repeated in the triplicate. The loading amount and loading efficiency were determined.

The loading efficiency (LE) was calculated by equation 1:

$$LE\%=((T-F)/T)*100 \quad (28) \qquad \text{(Eq. 1)}$$

And drug loading amounts (LA) were determined using equation 2:

$$LA\%=((T-F)/W)*100 \qquad \text{(Eq. 2)}$$

Where F is the free amount of drug in the supernatant, T is the total amount of drug added into the TiO_2-PEG NPs, and W is the weight of TiO_2-PEG-DOX NPs.

2.3. Characterization of TiO_2-PEG-DOX NPs

Particle size distribution and zeta potential of TiO_2-PEG-DOX NPs were analyzed using a laser diffraction particle size zeta potential analyzer (Microtrac, Nano-flex 180 °, USA) at room temperature. TiO_2-PEG-DOX NPs were prepared using PEG1000 or PEG4000 to investigate the effect of molecular weight of PEG on the dispersion of NPs.

For the analysis of drug release, TiO_2-PEG-DOX NPs were dispersed in 1.5 ml of buffer solution whose pH value was 7.4 or 5.0 in the micro-tubes. The tubes were put into shaker incubator (BIOER Mixing Block MB-102, China) and temperature was set to 37 °C. At scheduled time points, the NPs were separated by centrifugation at 10000 rpm for 10 min and the released drug in the supernatant was measured by HPLC method as described earlier. Following supernatant decantation, the same volume of fresh pre-warmed buffer solution was replaced. All measurements were performed in triplicate. The release percentage at each time was calculated and cumulative released curves were depicted.

2.4. Cytotoxicity assay

To verify the cytotoxicity of TiO_2-PEG-DOX, the cytotoxicity of TiO_2-PEG, DOX, and TiO_2-PEG-DOX was assessed by the standard MTT assay. Human breast cancer cell line (MCF-7) was purchased from the National Cell Bank of Pasteur Institute (Tehran, Iran). MCF-7 cells were cultured in CM10 medium supplemented with 10% fetal bovine serum and 1% penicillin streptomycin at 37 °C in a humidified incubator with 5% CO_2. Cells in the exponential growth phase were seeded in 96-well plates at a density of 1×10^4 viable cells/well. After overnight incubation, cells were exposed to different concentrations of TiO_2-PEG, DOX, and TiO_2-PEG-DOX. After 24 or 48 hr, 20 µL of MTT (5 mg/mL) and 100 µL of medium were introduced. The plates were incubated for 3-4 hr. The formazan crystals in each well were dissolved in 100 µL of dimethyl sulfoxide. After complete solubilization of the dye, plates were read at 570 nm against 690 nm on an ELISA reader. The percentage of cell viability was calculated. The cell viability was estimated as the reduction of values from a dimethyl sulfoxide control, and the values were the mean of three different experiments.

2.5. Statistical analysis

Data are expressed as mean±SD. Significant differences of the values were statistically tested using paired-sample t-test in each group. The statistical analyses were performed by SPSS® statistical software, version 20.0 (SPSS Inc., Chicago, IL, USA) for Windows®. A *P*-value of less than 0.05 was regarded as significant.

3. Result and Discussion

3.1. Characteristics of TiO2-PEG NPs

In this study, PEG with molecular weights of 400, 1000, and 4000 were used for coating the surface of TiO_2 NPs in order to improve the surface hydrophilicity, increase the half-life, and delay the clearance of these NPs. Among these three molecular weights, TiO_2 NPs coated with PEGs having molecular weight of 400 remained unstable and underwent agglomeration, and was excluded from the study because of sedimentation. However, TiO_2 NPs coated with PEGs having molecular weights of 1000 and 4000 were stable and produced a homogeneous and stable nano-suspension.

In order to investigate the TiO_2-PEG properties, TEM, DSC and TGA methods were used here. Based on the TEM results, the shape of all particles was almost uniform, and the formation of polymer layer around the TiO_2 NPs was obvious (Figure 1).

As shown in Figure 2a, in the DSC thermo-gram of PEG and TiO_2 physical mixture, an endothermic peak is observed at 92.62 °C, which is related to the PEG melting point. For TiO_2-PEG complex, this peak is shifted to 84.67 °C and becomes larger, which is related to the melting point of PEG and the evaporation of the water content of TiO_2. For PEG and TiO_2 physical mixture, three distinct exothermic peaks are observed at 237.47 °C, 173 °C, and 341.72 °C; the first two peaks are due to the phase change of TiO_2 from amorphous to anatase, and TiO_2 surface degradation and oxi-

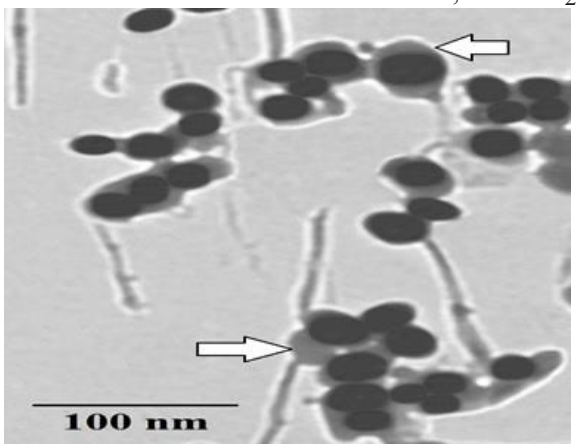

Figure 1. A TEM micrograph of TiO_2 NPs coated with PEG4000 (the arrow shows the PEG layer around the TiO_2 NPs).

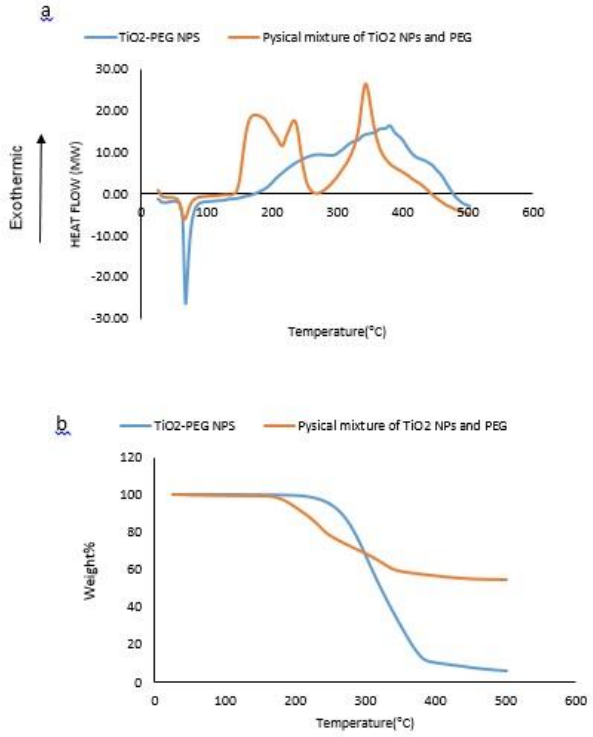

Figure 2. DSC (a) and TGA (b) thermograms of physical mixture of TiO_2 NPs and PEG, and TiO_2-PEG nano-composite.

dation; because the thermal behavior of TiO_2 depends on the chemical composition, preparation conditions, and phase. The 341.72 °C peak can be related to the chemical decomposition of PEG chains. When thermal behavior of TiO_2-PEG was examined, these distinct exothermic peaks were not observed; instead, a continuous peak started at 166 °C. Due to the presence of PEG chains on the surface of TiO_2, the phase change of these NPs is significantly reduced. Therefore, TiO_2 phase change peaks disappear after the PEG adsorption on the surface of these NPs. Thermal behavior after 300 °C in TiO_2-PEG refers to chemical decomposition of the polymeric chains on the surface of NPs.

In the TGA thermo-gram of PEG and TiO_2 physical mixture (figure 2b), weight loss occurs at two points. The first point is at 218.19 °C with a weight loss of 23%, and the second point is at 309 °C with a weight loss of 38%; these two phases correspond to the surface degradation of TiO_2 along with the loss of intermolecular water and eventually PEG decomposition. In the TiO_2-PEG thermo-gram, total weight loss is performed in a single stage at 312.23 °C, which is related to the chemical degradation of PEG chains. Finally, 6.5% of the material remains, indicating the TiO_2 NPs core.

3.2. Drug Loading

3.2.1. Effect of order of adding substances on the drug loading

In order to load DOX on the TiO_2-PEG NPs, two methods were tested according to the order of adding substances to each other. The results showed that when the drug was added to the TiO_2-PEG NPs, the loading efficiency was not changed compared to when the drug and the polymer were simultaneously added to the TiO_2 NPs. This indicates that PEG polymer does not play a role in drug loading of the TiO_2 NPs, and the interaction between DOX and TiO_2 NPs is effective in drug loading.

3.2.2. Effect of incubation duration time on the drug loading

Fluorescence spectroscopy was used to determine the incubation duration time effect on drug loading and was evaluated in 24 hr. The Fluorescence spectrum of DOX loaded on TiO_2-PEG NPs was completely different from the free drug. As shown in Figure 3, the interaction of DOX

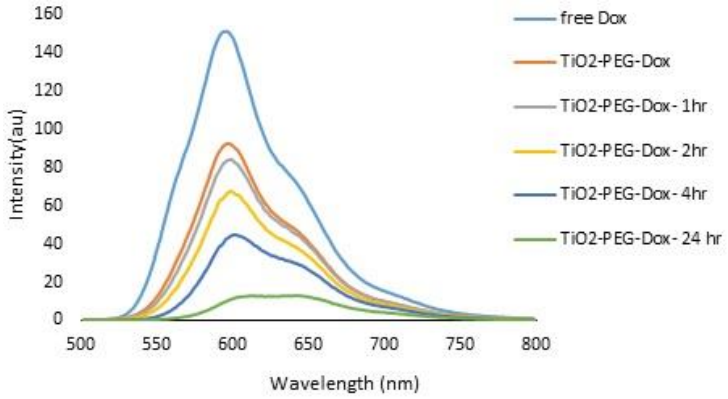

Figure 3. Fluorescence spectra of DOX reacted with TiO_2-PEG NPs for different times.

with TiO_2-PEG was accompanied by a significant reduction in the fluorescence absorption of DOX, while DOX molecules did not interact with each other, and a fluorescence absorption spectrum was observed from DOX solution. The results showed that by increasing the incubation time, the fluorescence absorption decreased until the drug loading reached saturation state after 24 hr.

3.2.3. Effect of DOX: TiO2 NPs weight ratio on the drug loading

According to Figure 4, the loading efficiency increased with increasing drug concentration, and after the saturation, it decreased PEG plays a role in separating TiO_2 NPs from each other and preventing their accumulation. The results of loading efficiency confirm this, because it was found that the efficiency of drug loaded on TiO_2-PEG4000 NPs was higher than TiO_2-PEG1000 (due to the greater ability of PEG4000 to disperse TiO_2 NPs and an increase in the available surface for drug loading). According to Figure 4, the highest efficiency for TiO_2-PEG4000 and TiO_2-PEG1000, was about 84% and 76%, respectively. These amounts are different significantly ($p<0.05$).

3.3. TiO2-PEG-DOX size and Zeta potential

In the optimum formulations with the highest loading efficiency, particle size and Zeta potential were analyzed. In TiO_2-PEG-DOX formulation, where PEG1000 was used to coat TiO_2 NPs, the mean volume diameter was 264.9 nm, while in TiO_2-PEG-DOX formulation, where PEG4000 was used, the mean volume diameter was 76 nm. Here, the better performance of PEG4000 in dispersing the NPs is confirmed again, and the larger size of TiO_2-PEG1000 is due to the accumulation of NPs. Moreover, the mean volume diameter of TiO_2-PEG4000 obtained by particle size analyzer was consistent with the results obtained from TEM technique.

The TiO_2-PEG-DOX Zeta potential lied in the positive range for both PEG molecular weights, while TiO_2 NPs had negative surface charge due to the presence of hydroxyl groups, the presence of positively charged DOX on the surface of these

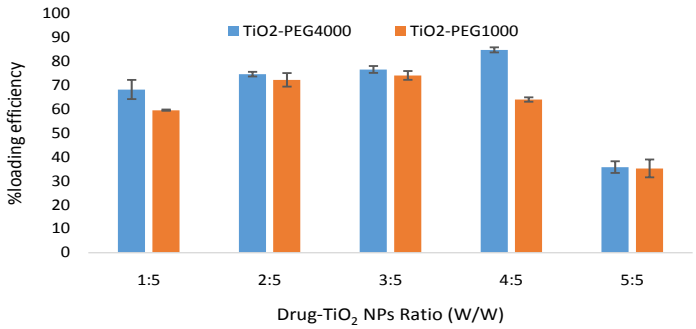

Figure 4. DOX loading efficiency on TiO_2-PEG1000 and TiO_2-PEG4000

metal NPs improved its Zeta potential, and the Zeta potential within the range appropriate for the stability of these particles. The Zeta potential of TiO_2-PEG1000-DOX is 12.6±0.56 and for TiO_2-PEG4000-DOX is 21.1±0.51.

3.4. Drug release

As shown in Figure 5, the drug release process in this study was investigated at two different pH levels. The profile of drug released shows that the drug release rate in acidic pH (pH 5) was higher than neutral pH (pH 7.4), which is a positive point for drug delivery to tumor cells and release in tumor cell lysosomes, but in general, the drug release from TiO_2-PEG NPs was insignificant. Despite the placement of NPs at different pH levels, the dilution of the release medium in order to break down the DOX and TiO_2 metal complex and also the use of external stress such as ultrasound waves, did not significantly change the drug release. This shows the stability of the interaction of TiO_2 with DOX. Nevertheless we found that stability cannot negatively affect the efficacy of the drug against cancer cells. In a similar study, a high release rate of this complex reported, while the loading efficiency was negligible and equal to 1.1% (21).

3.5. Effect of TiO2-PEG-DOX on cancer cell line

The cell cytotoxicity of TiO_2-PEG NPs, free DOX and TiO_2-PEG-DOX NPs against MCF-7 cell line was analyzed and present in Figure 6. TiO_2-PEG NPs alone did not have significant toxicity against MCF-7 cells. Comparison of the cytotoxicity effect of TiO_2-PEG-DOX with free DOX shows that after 24 hr' treatment, the effect of free DOX was higher, but after 48 hr, the effect of DOX loaded on TiO_2-PEG NPs was equivalent to that of free DOX and this effect was even greater in the concentration of 50 µg/mL of DOX ($p<0.05$). These data show that adsorption of DOX on the surface of TiO_2-PEG NPs does not eliminate the effect of the drug and even increases it to some extent, so that IC_{50} for free DOX was 39.8 µg/mL and for DOX loaded on the NPs was 31.6 µg/ml. This result indicates a gradual release of the drug in cancer cells. Despite the fact that the *in vitro* drug release was very low, the efficacy of the drug maintained and slightly increased in the cellular environment, due to the increased drug permeability in the cell in the presence of NPs.

4. Conclusion

It has been reported in previous studies that DOX has three potential metal binding sites: the nitrogen atom in the sugar moiety, and the

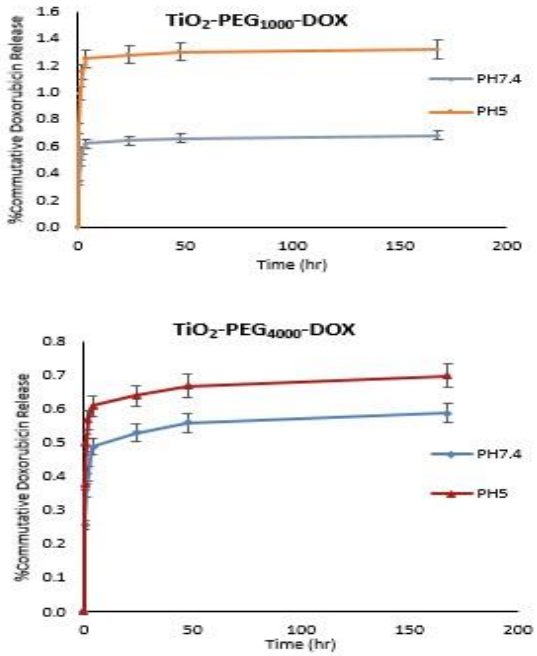

Figure 5. DOX release profile from TiO_2-PEG1000 and TiO_2-PEG4000 at pH 5 and pH 7.4.

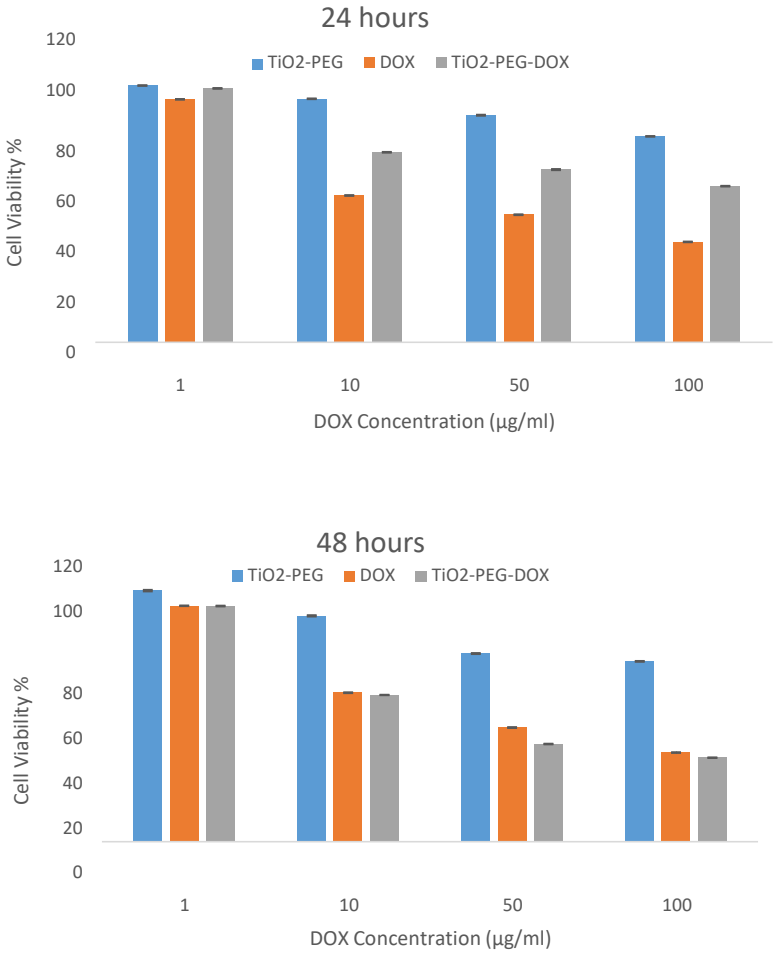

Figure 6. Cell cytotoxicity assay of TiO_2-PEG-DOX NPs against MCF-7 cells with different treatments for 24 and 48 hr.

chelating sites of the quinone, and the phenolic oxygens on both sides of the anthracycline aromatic moiety (28). It is established that two keto-phenolate functions are the major sites for making complex with some metal ions like Ca^{2+}, Mg^{2+}, Zn^{2+} , Ni^{2+} (28). Chen *et al.* indicated that DOX can be easily adsorbed onto the surface of TiO_2 NPs via electrostatic interaction (23). In this study, the fluorescence spectra of DOX-loaded TiO_2 NPs indicated this interaction. The fluorescence spectra of TiO_2-PEG-DOX showed significant differences from that of free DOX. The interaction of DOX with TiO_2 NPs was indicated by a sharp quenching of DOX fluorescence in the presence of TiO_2 NPs, whereas self-quenching of pure DOX was not observed (Figure 3).

The addition of PEG to the surface of TiO_2 NPs may decrease the interaction of NPs and avoid sedimentation of these NPs in the aqueous media. In addition, this hydrophilic polymer can avoid the rapid clearance of nano-materials by RESs, and greatly increases their blood half-life and therefore enhances the accumulation of nanoparticles in the tumor site (29-31).

Cytotoxicity assay was performed against MCF-7 cells in the present study. When the cells were treated with TiO_2 NPs at high concentrations, after 48 hr, about 80% of the cells survived (Figure 6). This result suggests lack of major cytotoxicity for TiO_2 NPs, which is consistent with other reports. This is an acceptable property for a carrier in drug delivery systems. Our results also showed a dose-dependent effect of free DOX and DOX loaded TiO_2 NPs *in vitro*. We observed that the IC_{50} for free DOX was 39.8 µg/mL and for DOX loaded on the NPs was 31.6 µg/mL. TiO_2 NPs can improve cellular uptake of DOX through the endocytosis pathway, which is a positive point in the

drug delivery systems based on NPs. Chen *et al.* showed that the IC_{50} value for free DOX against human hepatocarcinoma SMMC-7721 cell line was 0.32 µg/mL, and for DOX-TiO_2 NPs was 0.20 µg/mL (23). The lower IC_{50} for the DOX loaded TiO_2 NPs could improve the therapeutic efficacy-while decreasing the toxic side effects. The characteristics of TiO_2-PEG-DOX show that this drug delivery system is a promising strategy for future clinical practice.

Acknowledgments

This work was financially supported by Shiraz University of Medical Sciences (Grant No. 13652).

Conflict of Interest

None declared.

5. References

1. Bertrand N, Leroux J-CC. The journey of a drug-carrier in the body: An anatomo-physiological perspective. *J Control Release.* 2012 Jul 20;161(2):152-63.
2. Yin ZF, Wu L, Yang HG, Su YH. Recent progress in biomedical applications of titanium dioxide. *Phys Chem Chem Phys.* 2013;15(14):4844-58.
3. Du Y, Ren W, Li Y, Zhang Q, Zeng L, Chi C, et al. The enhanced chemotherapeutic effects of doxorubicin loaded PEG coated TiO2 nanocarriers in an orthotopic breast tumor bearing mouse model. *J Mater Chem B.* 2015;3(8):1518-28.
4. Yakunin AN, Avetisyan Y a., Tuchin V V. Quantification of laser local hyperthermia induced by gold plasmonic nanoparticles. *J Biomed Opt.* 2015;20(5):051030.
5. Behnam MA, Emami F, Sobhani Z, Koohi-Hosseinabadi O, Dehghanian AR, Zebarjad SM, et al. Novel combination of silver nanoparticles and carbon nanotubes for plasmonic photo thermal therapy in melanoma cancer model. *Adv Pharm Bull.* 2018;8(1).
6. Thompson EA, Graham E, MacNeill CM, Young M, Donati G, Wailes EM, et al. Differential response of MCF7, MDA-MB-231, and MCF 10A cells to hyperthermia, silver nanoparticles and silver nanoparticle-induced photothermal therapy. *Int J Hyperth*. 2014 Aug;30(5):312-23.
7. Sobhani Z, Behnam MA, Emami F, Dehghanian A, Jamhiri I. Photothermal therapy of melanoma tumor using multiwalled carbon nanotubes. *Int J Nanomedicine.* 2017 Jun;12:4509-17.
8. Behnam MA, Emami F, Sobhani Z, Dehghanian AR. The application of titanium dioxide (TiO2) nanoparticles in the photo-thermal therapy of melanoma cancer model. *Iran J Basic Med Sci.* 2018;21(11):1133-9.
9. Jhuang Y-Y, Cheng W-T. Fabrication and characterization of silver/titanium dioxide composite nanoparticles in ethylene glycol with alkaline solution through sonochemical process. *Ultrason Sonochem.* 2016 Jan;28:327-33.
10. Eskandarloo H, Badiei A, Behnajady MA, Ziarani GM. Ultrasonic-assisted sol-gel synthesis of samarium, cerium co-doped TiO2 nanoparticles with enhanced sonocatalytic efficiency. *Ultrason Sonochem.* 2015;26:281-92.
11. Jugan ML, Barillet S, Simon-Deckers A, Sauvaigo S, Douki T, Herlin N, et al. Cytotoxic and Genotoxic Impact of TiO2 Nanoparticles on A549 Cells. *J Biomed Nanotechnol.* 2011 Jan 1;7(1):22-3. age=22
12. Carp O, Huisman CL, Reller a. Photoinduced reactivity of titanium dioxide. *Prog Solid State Chem.* 2004;32(1-2):33-177.
13. Haseeb ASMA, Hasan MM, Masjuki HH. Structural and mechanical properties of nanostructured TiO2 thin films deposited by RF sputtering. *Surf Coatings Technol.* 2010;205(2):338-44.
14. He Q, Wen X, Ma P, Deng X. Alkali induced morphology and property improvements of TiO2 by hydrothermal treatment. *J Wuhan Univ Technol Mater Sci Ed.* 2008;23(4):503-6.
15. Ratner, D.B.; Brunette, D.M.; Tengvall, P.; Textor, M.; Thomsen P. Titanium in Medicine, Proceedings of the Institution of Mechanical Engineers, Part H: Journal of Engineering in Medicine, vol. 216, 3: pp. 215. , First Published Mar 1, 2002
16. Devanand Venkatasubbu G, Ramasamy S, Ramakrishnan V, Kumar J. Folate targeted PEGylated titanium dioxide nanoparticles as a nanocarrier for targeted paclitaxel drug delivery. *Adv Powder Technol.* 2013 Nov;24(6):947-54.
17. Moosavi Nejad S, Takahashi H, Hosseini H, Watanabe A, Endo H, Narihira K, et al. Acute effects of sono-activated photocatalytic titanium dioxide nanoparticles on oral squamous cell carcinoma. *Ultrason Sonochem.* 2016;32:95-101.

18. Yamaguchi S, Kobayashi H, Narita T, Kanehira K, Sonezaki S, Kudo N, et al. Sono-dynamic therapy using water-dispersed TiO2-polyethylene glycol compound on glioma cells: Comparison of cytotoxic mechanism with photodynamic therapy. *Ultrason Sonochem.* 2011;18(5):1197-204.
19. Wang R, Hashimoto K, Fujishima A, Chikuni M, Kojima E, Kitamura A, et al. Light-induced amphiphilic surfaces. Nature. 1997;388:431–2.
20. Xu P, Wang R, Ouyang J, Chen B. A new strategy for TiO2 whiskers mediated multi-mode cancer treatment. *Nanoscale Res Lett.* 2015;10:94.
21. Ren W, Zeng L, Shen Z, Xiang L, Gong A, Zhang J, et al. Enhanced doxorubicin transport to multidrug resistant breast cancer cells via TiO2 nanocarriers. *RSC Adv.* 2013;3(43):20855-61.
22. Liu E, Zhou Y, Liu Z, Li J, Zhang D, Chen J, et al. Cisplatin Loaded Hyaluronic Acid Modified TiO 2 Nanoparticles for Neoadjuvant Chemotherapy of Ovarian Cancer. *J Nanomater.* 2015;2015:1-8.
23. Jiao Z, Chen Y, Wan Y, Zhang H, Wang Y, Zhang H, et al. Anticancer efficacy enhancement and attenuation of side effects of doxorubicin with titanium dioxide nanoparticles. *Int J Nanomedicine.* 2011 Oct;6:2321.
24. Szaciłowski K, Macyk W, Drzewiecka-Matuszek A, Brindell M, Stochel G. Bioinorganic Photochemistry: Frontiers and Mechanisms. *Chem Rev*. 2005 Jun;105(6):2647-94.
25. Song M, Zhang R, Dai Y, Gao F, Chi H, Lv G, et al. The in vitro inhibition of multi-drug resistance by combined nanoparticulate titanium dioxide and UV irradition. *Biomaterials.* 2006;27(23):4230-8.
26. Cai R, Kubota Y, Shuin T, Sakai H, Hashimoto K, Fujishima A. Induction of Cytotoxicity by Photoexcited TiO2 Particles. *Cancer Res.* 1992;52(8):2346-8.
27. Furuzono T, Iwasaki M, Yasuda S, Koremastu A, Yoshioka T, Ito S, et al. Photoreactivity and cell adhesiveness of amino-group-modified titanium dioxide nano-particles on silicone substrate coated by covalent linkage. *J Mater Sci Lett.* 2003;22(24):1737-40.
28. Barick KC, Nigam S, Bahadur D. Nanoscale assembly of mesoporous ZnO: A potential drug carrier. *J Mater Chem.* 2010;20(31):6446-52.
29. Li G, Li L, Boerio-Goates J, Woodfield BF. High purity anatase TiO2 nanocrystals: Near room-temperature synthesis, grain growth kinetics, and surface hydration chemistry. *J Am Chem Soc*. 2005;127(24):8659-66.
30. Jaroenworaluck A, Sunsaneeyametha W, Kosachan N, Stevens R. Characteristics of silica-coated TiO2 and its UV absorption for sunscreen cosmetic applications. *In: Surface and Interface Analysis*. 2006. p. 473-7.
31. Liu E, Zhou Y, Liu Z, Li J, Zhang D, Chen J, et al. Cisplatin loaded hyaluronic acid modified TiO2 nanoparticles for neoadjuvant chemotherapy of ovarian cancer. *J Nanomater.* 2015;2015: 1-8.